International Journal of River Basin Management

ISSN: (Print) (Online) Journal homepage: www.tandfonline.com/journals/trbm20

Identification of flood-prone areas in Kaziranga National Park, Assam, India

Shehnaj Ahmed Pathan & Gwakulo Tep

To cite this article: Shehnaj Ahmed Pathan & Gwakulo Tep (12 Mar 2025): Identification of flood-prone areas in Kaziranga National Park, Assam, India, International Journal of River Basin Management, DOI: 10.1080/15715124.2025.2477161

To link to this article: https://doi.org/10.1080/15715124.2025.2477161

Published online: 12 Mar 2025.

INTERNATIONAL JOURNAL OF RIVER BASIN MANAGEMENT
https://doi.org/10.1080/15715124.2025.2477161

Taylor & Francis
Taylor & Francis Group

Identification of flood-prone areas in Kaziranga National Park, Assam, India

Shehnaj Ahmed Pathan and Gwakulo Tep

Department of Civil Engineering, The Assam Kaziranga University, Jorhat, India

ABSTRACT

Flooding poses a significant challenge in arid and semi-arid regions, where unexpected rainfall can cause catastrophic consequences. Kaziranga National Park, a UNESCO World Heritage Site in Assam, faces annual floods threatening its rich biodiversity, particularly the iconic one-horned rhinoceroses. Therefore, assessing flood risk in this region to save the animals is of utmost importance. This study assessed flood-prone zones in Kaziranga for 2015 and 2019 using GIS-based multi-criteria analysis. Factors like flow accumulation, slope, soil type, land use, rainfall intensity and elevation were integrated to map flood risk areas. The results indicated that the northeastern parts of the park had the highest flood vulnerability, with flood risk significantly increasing in 2019 compared to 2015. High and very high flood-prone areas covered 36.83% and 31.26% of the study area in 2019. Rainfall and soil type were the most influential factors, with clayey soils on the northern side near the Brahmaputra River intensifying runoff, while sandy soils in the southern region reduced flood risk due to higher infiltration. The study highlights the need for strategic flood mitigation measures to protect the park's wildlife. These findings offer valuable insights for conservation planning, aiding authorities in minimizing flood impacts and safeguarding Kaziranga's unique ecosystem.

ARTICLE HISTORY
Received 9 August 2023
Accepted 5 March 2025

KEYWORDS
Kaziranga National Park; Brahmaputra River; weighting overlay; flood; one-horned rhino

Introduction

Floods are among the most widespread and devastating natural hazards affecting river basins across the globe, with severe social, economic, and environmental consequences. Flooding occurs when rivers exceed their capacity, leading to the inundation of nearby low-lying areas. The increasing frequency and severity of floods, driven by climate change and intensified rainfall, have drastically impacted ecosystems and human communities, resulting in significant loss of life, property destruction, and disruptions to agriculture, infrastructure, and water quality. Rapid population growth, urbanization, and infrastructure development have further heightened the exposure of communities to flood hazards, especially in the face of extreme weather events (James and Hall 1986, Kron *et al.* 2019). Given the importance of flood management, numerous researchers have explored methods for delineating flood-prone zones, predicting flash floods, and developing flood risk assessments. Various studies have utilized a range of models and techniques, spanning from localized analyses to extensive regional assessments, to understand and address flood risks (Sinha *et al.* 2008, Emmanuel Udo *et al.* 2015, Adlyansah *et al.* 2019, Thapa *et al.* 2020, Malgwi *et al.* 2021, Bento *et al.* 2023, Fagunloye 2024). Regional insights are often best visualized through maps, which play a crucial role in providing actionable information for decision-makers to optimize disaster preparedness and response strategies (Mase 2020). The application of Geographic Information System (GIS) tools has proven particularly effective in generating thematic maps that identify flood-vulnerable areas (Wang *et al.* 2011). Numerous studies have employed GIS-based techniques to integrate factors like flow accumulation, slope, land use, and precipitation, enabling comprehensive flood risk assessments (Bapalu and Sinha 2005, Erena and Worku 2018, Ashwini *et al.* 2020). These maps provide essential resources for proactive planning, helping mitigate flooding impacts. Several methodologies have been developed for flood hazard zoning. Kourgialas and Karatzas (2011) proposed an approach aligned with the European Floods Directive, focusing on parameters such as flow accumulation, slope, rainfall intensity, and land use. Advanced models like weighted overlay and fuzzy AHP decision-making methods have also been utilized, incorporating layers such as digital elevation models (DEM), normalized difference vegetation index (NDVI), and hydrological factors (Ouma and Tateishi 2014, Ozkan and Tarhan 2016, Hasanloo *et al.* 2019). Recent advancements have emphasized GIS-based multi-criteria decision analysis (MCDA). Studies by Ajjur and Mogheir (2020), Kumar and Jha (2023), and Osman and Das (2023) effectively integrated criteria like drainage network proximity, elevation, and land use to assess flood risks. Factors such as altitude, flow accumulation, slope, precipitation, and land use consistently emerge as significant determinants of flood risks, irrespective of the study area's characteristics (Hagos *et al.* 2022, Enomah *et al.* 2024). In India, Kumar and Sen (2022) classified flood-prone areas of the Deoha River basin using weighted overlay analysis. Ghosh *et al.* (2023) created an integrated framework to assess flood susceptibility, vulnerability, and risk in Malda District through RS and GIS-based AHP methodologies. Similarly, Mohammed *et al.* (2024) mapped flood hazards in the Diyala governorate, incorporating nine factors, including elevation, slope, drainage density, NDVI, and topographic wetness index. These studies demonstrate the importance of GIS-based techniques and multi-criteria approaches in flood risk assessment and mitigation planning. Despite significant advancements in flood risk assessments, there is a notable gap in research that integrates soil type with other hydrological and

CONTACT Shehnaj Ahmed Pathan shehnajpathan9@gmail.com Department of Civil Engineering, The Assam Kaziranga University, Jorhat, 785006, India

topographical factors, such as altitude, slope, flow accumulation, precipitation, and land use, particularly in ecologically sensitive regions like Kaziranga National Park. The interaction between soil properties and hydrological factors plays a crucial role in flood dynamics, influencing infiltration, runoff, and water retention. While studies have explored soil characteristics and their impact on flood behavior, such analyses are scarce in protected areas like Kaziranga. Soil properties, including infiltration rates and water retention capacity, are fundamental to understanding flood dynamics, yet they are often underutilized in flood risk studies. Moreover, the application of hydrological-hydraulic models in data-scarce regions, particularly in developing countries like India, remains a significant challenge due to limitations in GIS resources and data availability. These constraints highlight the need for scalable, adaptable methodologies capable of operating with available data while providing accurate, location-specific flood risk assessments (Figure 1).

In Assam, floods are a recurring natural event, particularly during the monsoon season when the Brahmaputra River overflows. This annual flooding severely impacts Kaziranga National Park (KNP), which is located on the southern bank of the river. Each year, nearly 70% of the park becomes submerged, creating challenges for the wildlife that inhabits the area. Flooding occurs frequently throughout the monsoon season (April-September) of every year. The Brahmaputra River serves as the park's immediate boundary, so when it floods, the extra water covers 80–90% of the entire area. The flood water severely impacts the wildlife of the region for at least 10–20 days (Figure 2). Floods in Kaziranga have caused significant wildlife mortality, notably during the 1998 floods, with 39 rhinos, 23 wild water buffalo, 19 wild pigs, and 15 sambars drowned. Hog deer were severely affected, with 473 deaths recorded. Populations of deer and wild pigs declined sharply between 1984 and 1991, from 10,000 to 2,900 deer and 1,645 to 555 wild pigs (Mathur *et al.* 2005).

Flooding in Kaziranga National Park, though essential for maintaining its fertile ecosystem, significantly impacts its vulnerable wildlife. Rising floodwaters force animals such as hog deer, one-horned rhinos, and elephants to seek higher ground, primarily in the Karbi Anglong Hills. During this migration, many animals drown, while others fall victim to human-wildlife conflict upon entering nearby villages for refuge. National Highway 37, running through the park, exacerbates the situation. Animals crossing the highway to reach safety are frequently struck by vehicles, leading to fatalities. Additionally, poaching incidents increase during floods, as weakened anti-poaching infrastructure, including damaged patrol paths, roads, and guard camps, creates enforcement gaps. Flooding also forces animals out of protected areas into densely populated regions, complicating conservation efforts and increasing the risk of poaching, road accidents, and human-animal conflict. This annual cycle of displacement severely disrupts wildlife safety, while the destruction of anti-poaching infrastructure hinders the park's ability to respond effectively. Identifying flood-prone areas within the park and implementing mitigation measures – such as elevated wildlife corridors, improved monitoring systems, and community awareness programs – are critical to reducing these adverse impacts and safeguarding Kaziranga's biodiversity during flood events. This annual cycle of flooding highlights the urgent need for improved measures

Figure 1. A few recent photographs of Kaziranga National Park taken by the author in the year January, 2024 during the dry season.

Figure 2. A few recent photographs of Kaziranga National Park taken by the author from the national highway in the year July 2024 during the flood.

to protect the park's wildlife, such as creating safer passages for animals during floods and enhancing monitoring systems to prevent accidents and human-animal conflict. Some research related to Kaziranga National Park has been done on different topics. Ghosh *et al.* (2018) employed remotely sensed satellite data to rapidly assess the occurrence of recent floods in Kaziranga National Park, Assam. Borah *et al.* (2018) aimed to utilize SAR (Synthetic Aperture Radar) data for flood monitoring in Kaziranga National Park. Data limitations, like sparse stream gauges or short rainfall measurement intervals, hinder precise flood assessments in Kaziranga National Park. However, no detailed study related to identifying flood-prone areas has been conducted. Hence, the main aim of this study is to delineate a flood-prone map, identify the locations at high risk of flooding, and find out the factors that influence these areas to develop efficient conservation strategies in Kaziranga National Park.

Study area and input data

The research focuses on Kaziranga National Park (KNP), located in the floodplain of the Brahmaputra River, bounded by the geographical coordinates of approximately latitude 26°35′ to 26°45′ N and longitude 93°05′ to 93°40′ E. The national park encompasses portions of Nagaon and Golaghat districts in Assam, India, spanning an area of approximately 430 square kilometers along the southern side of the Brahmaputra River (Figure 3). KNP is renowned worldwide for its one-horned Rhinoceros population. Indeed, Kaziranga National Park extends from the Brahmaputra River in the northern part to National Highway No. 37 in the south. The park is encircled by the highway along its southern boundary, located at the foothills of the Karbi Anglong hills (Kushwaha *et al.* 2000). Just outside the park's southern edge is Panbari Forest, a tiny but significant location for

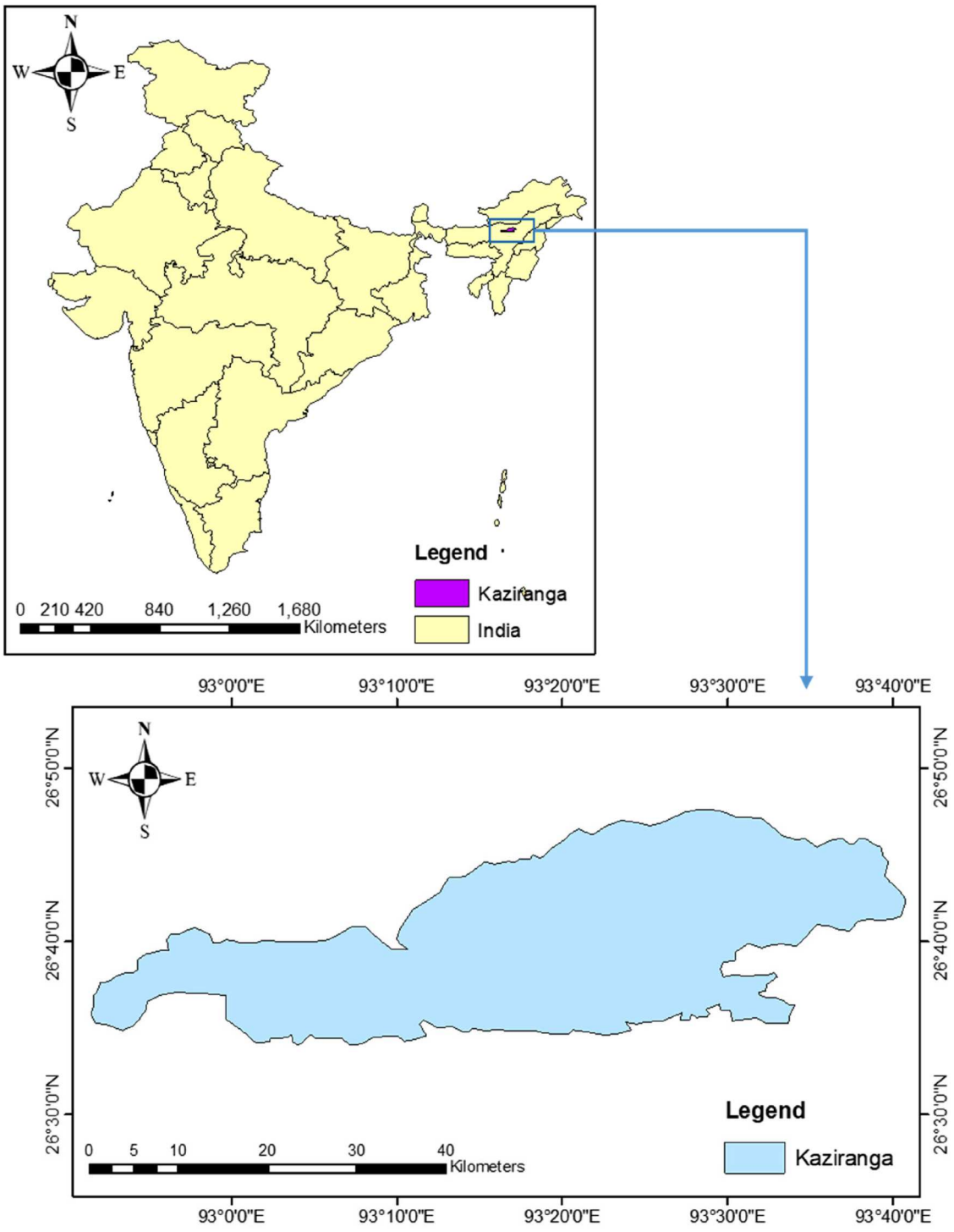

Figure 3. Location map of the study area within Kaziranga National Park (KNP).

many forest species (Sinha *et al.* 2011). For recording purposes, Kaziranga is occasionally combined with Panbari Forest. The study area encompasses several ranges, including the Agaratoli range, Kohora range, Bagori, and Burapahar range (Medhi and Sakia 2019). The terrain within the park is predominantly flat, with an elevation ranging from 55 to 75 meters above mean sea level (MSL), sloping gently from east to west (Patnaik *et al.* 2019). In Rodger *et al.*'s (2002) study, Kaziranga National Park is described as having a typical subtropical monsoon climate. From east to west, the park is traversed by a number of tiny rivers and channels, some of which rise in the Karbi Anglong highlands to the south and eventually flow north to join the Brahmaputra River (Barua and Sharma 1999). Older channels have been preserved as shallow oxbow lakes, or 'beels', in the area. Within the park, there are at least nine such beels that range in size from 50 to 150 acres. Kaziranga National Park consists of four primary habitats: grasslands, forest cover, wetlands, and sand depositions (Kushwaha and Unni 1986). The Brahmaputra River's floodplain gives the park's soil a rich alluvial deposit history. Swamps and marshes have formed as a result of some beels silting up. As a result, there are now more regions with tall grass and fewer areas with low grass. In the future, this progressive transformation will have significant ecological ramifications. A yearly occurrence, floods overwhelm the area with extra water, covering 50–70% of the whole landmass (Barua and Sharma 1999). After 7–10 days, the flood waters usually start to recede. At a higher

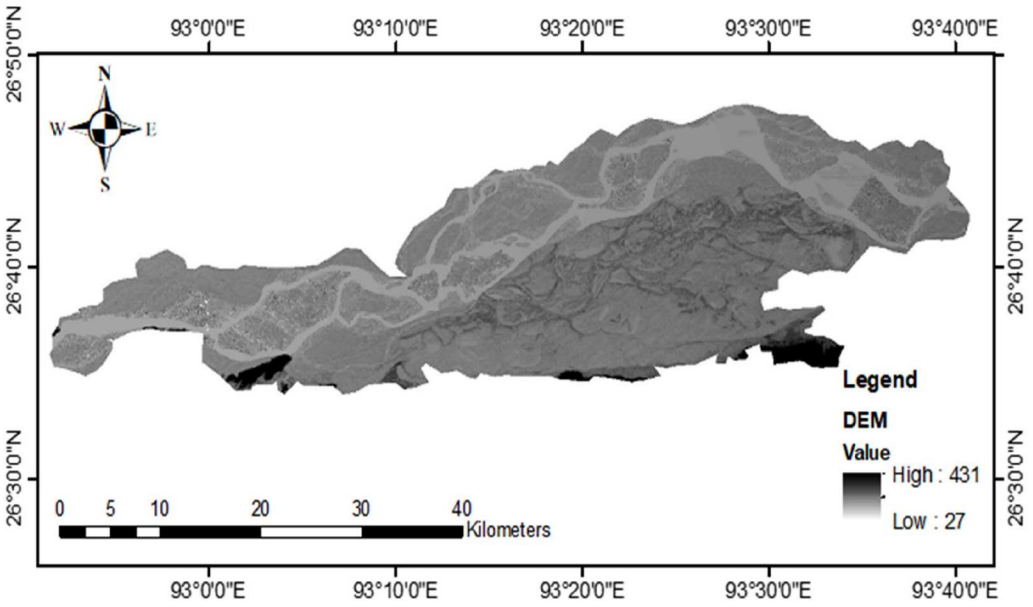

Figure 4. Digital Elevation Model Map of Kaziranga National Park.

height (80–100 m above MSL), the areas along the foothills of Karbi Anglong hills produce naturally occurring 'highlands' that do not flood. The Brahmaputra River's erosion and movement cause a continuous alteration in the overall area. Kaziranga National Park boundary area is extracted by georeferencing from the image found in a study done by Medhi and Sakia (2019).

The Digital Elevation Model (DEM) data utilized in the study has a resolution of 30 meters (1 Arc Second), which has been downloaded from the website https://lpdaac.usgs.gov/ (Figure 4). Soil map of the study area is downloaded from FAO Digital Soil Map of the World (Figure 5). Due to data availability constraints, this study could obtain Land Use and Land Cover (LULC) data for only two years, namely 2015 and 2019. The downloaded data comes with a good resolution of 100 m Land Cover products, covering the retrieval methodology sourced from Copernicus Global Land Service. LULC maps of 30-meter resolution were prepared from the downloaded data, as shown in Figure 6. Gridded Rainfall data for 2015 and 2019 is downloaded from Climate Forecast System Reanalysis (CFSR). A total of ten gridded stations are found within the study area (Figure 7). The Longitude, Latitude, and Elevation of all the gridded points are mentioned in Table 1.

Methodology

Flood risk maps are crucial for land use planning in flood-prone areas, integrating flood return periods, water depths, and hydrological factors to assess flood susceptibility. Their development follows four key phases: hydrologic, geomorphic, hydraulic, and land use analysis, utilizing ArcGIS for accurate mapping. A vital data source is Digital Elevation Model (DEM)

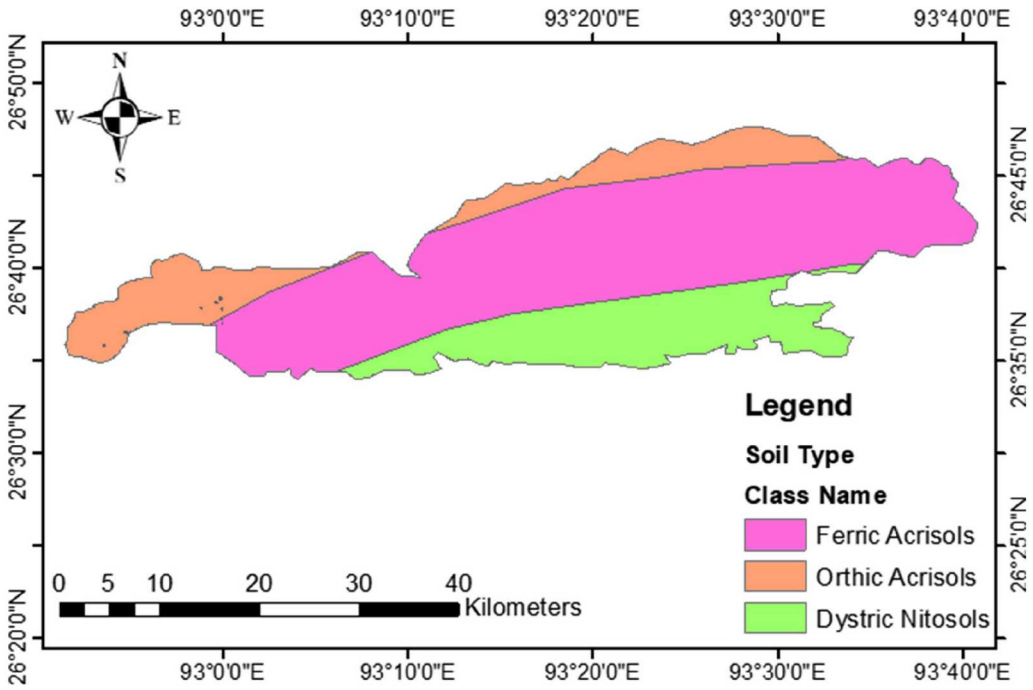

Figure 5. Soil map of Kaziranga National Park.

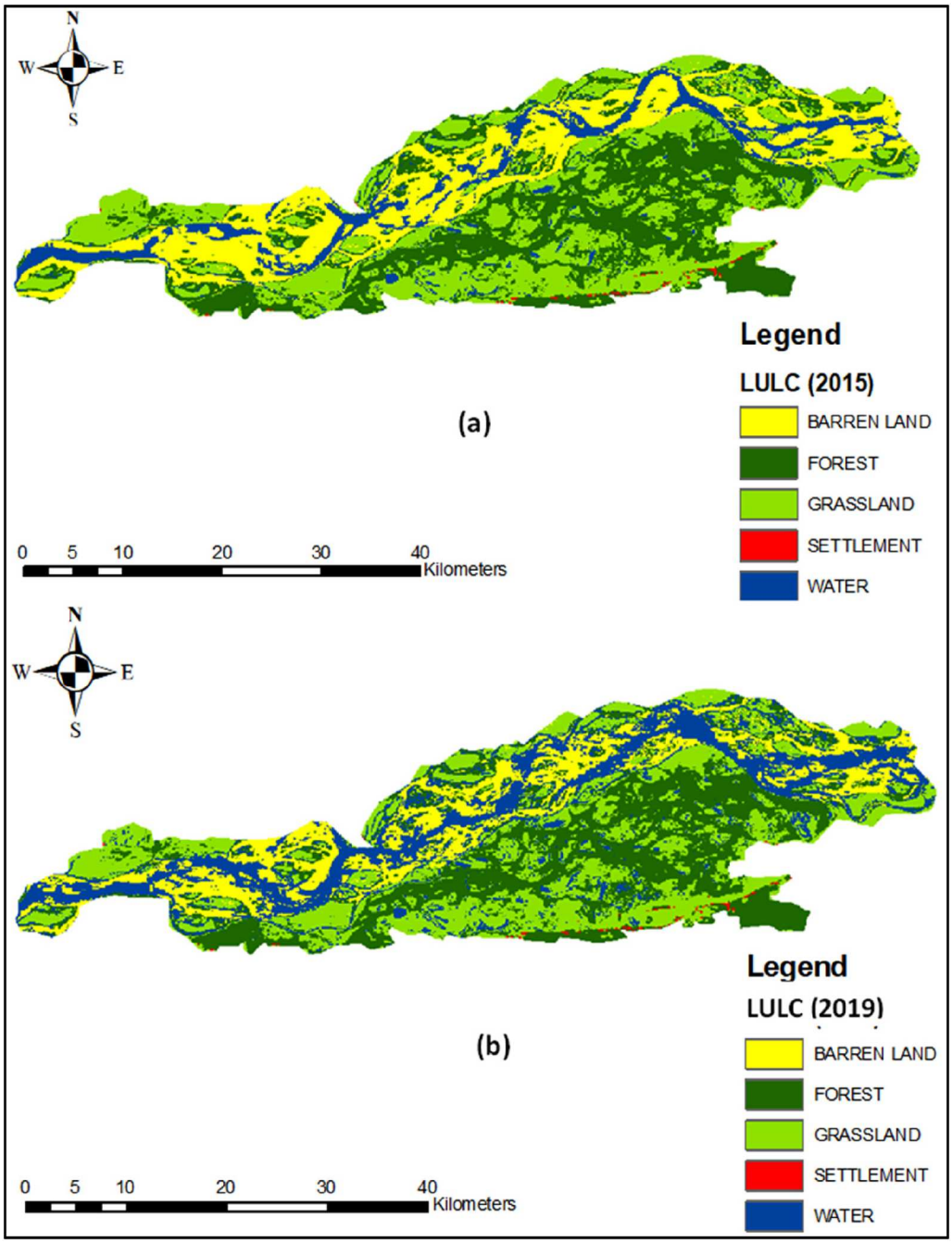

Figure 6. Land Use/ Land Cover maps of Kaziranga National Park for the years (a) 2015 and (b) 2019.

data, which aids in calculating flow direction and accumulation, defining drainage areas, and outlining water flow boundaries. Flow accumulation estimates drainage areas in raster units (Ozkan and Tarhan 2016). Rainfall intensity, Land Use/Land Cover (LULC), and soil type are critical in flash flood generation, particularly in small river basins (Belmonte and Beltran, 2001). Soil moisture, influenced by vegetation, affects precipitation infiltration, while soil type regulates runoff. The curve number (CN) method effectively links runoff to land use, soil moisture, and rainfall intensity, significantly impacting flood formation (Svoboda 1991). This study integrates six key factors – precipitation, slope, flow accumulation, elevation, soil characteristics, and LULC – to comprehensively assess flood risk. The study integrates multiple data sources to generate thematic layers for flood risk assessment. Precipitation Data: Collected from meteorological stations and interpolated using the Inverse Distance Weighted (IDW) method to create a raster surface representing spatial rainfall distribution. Topographic Data: Digital Elevation Model (DEM) data is used to derive slope, elevation, flow direction, and flow accumulation maps. Soil Data: Soil classification maps are used to analyze soil infiltration rates, which influence runoff dynamics. LULC Data: Land cover and land use maps at a 30 m resolution for 2015 and 2019 are analyzed to identify impervious and pervious surfaces affecting flood susceptibility. Each factor influencing flood risk is processed in ArcGIS using specialized geoprocessing tools:

Precipitation Analysis: Rainfall is a primary driver of flooding. Higher precipitation levels correlate with more significant flood risks. The rainfall data is interpolated using the inverse weighted distance (IDW) method, creating a raster surface that accurately depicts rainfall amounts. IDW interpolation is recommended because it is the most suitable method for studies with a limited number of examples, just

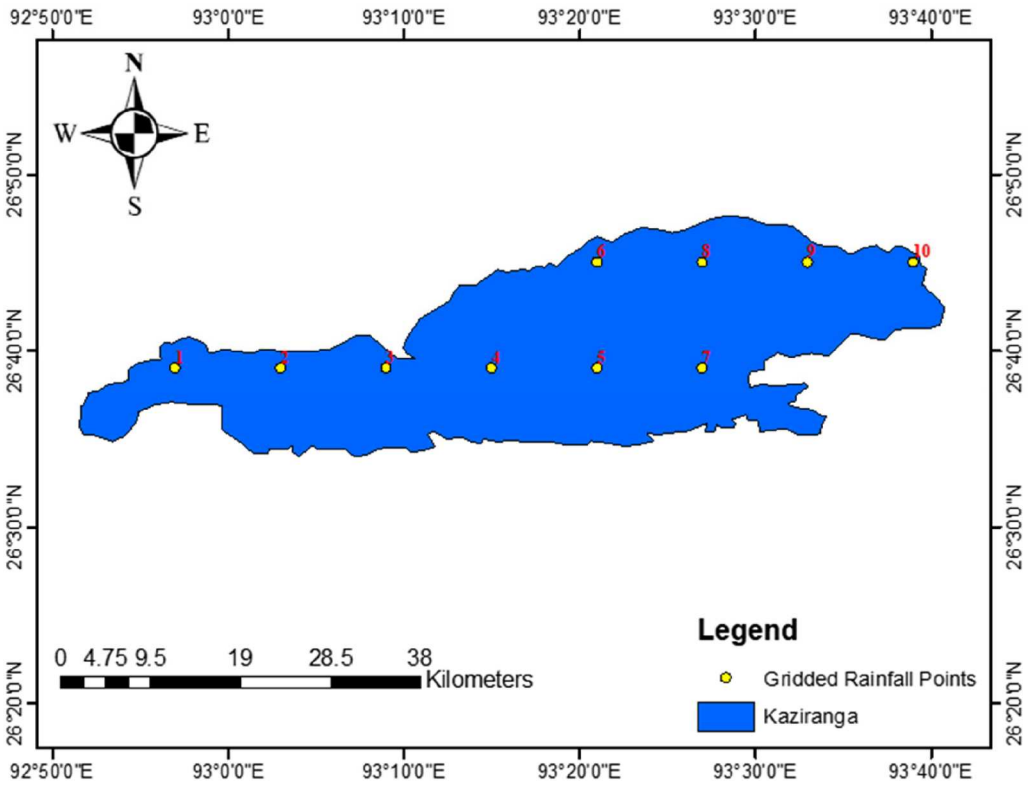

Figure 7. Gridded rainfall points map within Kaziranga National Park.

Table 1. Gridded rainfall points with their Longitude, Latitude, and Elevation for Kaziranga National Park.

Gridded Rainfall Points	Longitude (in degree)	Latitude (in degree)	Elevation (m)
1	92.95	26.65	71
2	93.05	26.65	64
3	93.15	26.65	61
4	93.25	26.65	67
5	93.35	26.65	79
6	93.35	26.75	71
7	93.45	26.65	80
8	93.45	26.75	76
9	93.55	26.75	76
10	93.65	26.75	77

like the study region. Higher precipitation levels indicate higher levels of flood risk and vice versa. Slope Analysis: The slope of the terrain significantly affects water movement and flood risks. Steeper slopes facilitate rapid runoff, reducing infiltration time, whereas gentler slopes are more prone to flooding. To calculate the slope of KNP, the steepness of each elevation raster cell is determined. The slope is calculated from the DEM, and areas are classified into hazard levels using Jenks Natural Breaks classification. A collection of tools from the ArcGIS toolbox will be utilized, specifically for tasks such as flow direction, downslope analysis, and flow accumulation (in the case of rainfall) can be taken into consideration. Flow accumulation refers to the sum of the weights of all cells that flow downslope into each output raster cell (Babalola and Abilodun 2019). Cells with higher accumulation values indicate concentrated flow patterns, which, in turn, escalate the risk of flooding in those areas. The slope is another factor for flood hazards in flat and low-elevation locations. As the surface slope rises, the risk of floods grows (Eini *et al.* 2020). Additionally, places with steep slopes speed up water flow and shorten the time it takes for water to permeate and absorb into the earth. This is consistent with the idea that a steeper slope indicates a lower flood risk level than a gentle slope suggests a higher risk of flooding. Low-lying areas are more vulnerable to flooding. The DEM is processed to classify elevation into five flood risk categories using Jenks Natural Breaks.

Soil type constitutes another significant factor influencing the likelihood of flooding. Soil properties influence runoff generation. Sandy soils allow greater infiltration, reducing flood risks, while clayey and compacted soils promote surface runoff. Soil maps are classified based on permeability and integrated into the flood risk model. Land use documentation pertains to how individuals utilize the land, while land cover delineates the physical features of the land, such as forests or open water bodies (Bartalev *et al.* 2003). LULC analysis is essential for assessing flood risk, as areas with dense vegetation are less prone to flooding due to increased water absorption. Conversely, impervious surfaces, such as urban areas, significantly heighten flood susceptibility. This study utilizes LULC maps from 2015 and 2019 at a 30-meter resolution. Areas are classified into developed (impervious) and undeveloped (pervious) categories to assess flood risk distribution. The proximity of water bodies to other land areas within the study region is also considered, as closer distances indicate higher flood vulnerability. Figure 8 illustrates the flow chart for flood risk assessments in more detail.

To quantify flood susceptibility, a weighted overlay method is applied. The methodology follows Assefa (2018) and Shaban *et al.* (2001) in assigning weights to factors based on their relative influence on flood hazards. In this study, six key factors are used. These factors vary in their degree of influence, and the analysis accounts for both direct (primary) and indirect (secondary) effects of one factor on another. To assign weights, each factor's interactions with other factors are carefully analyzed. Solid lines in Figure 9

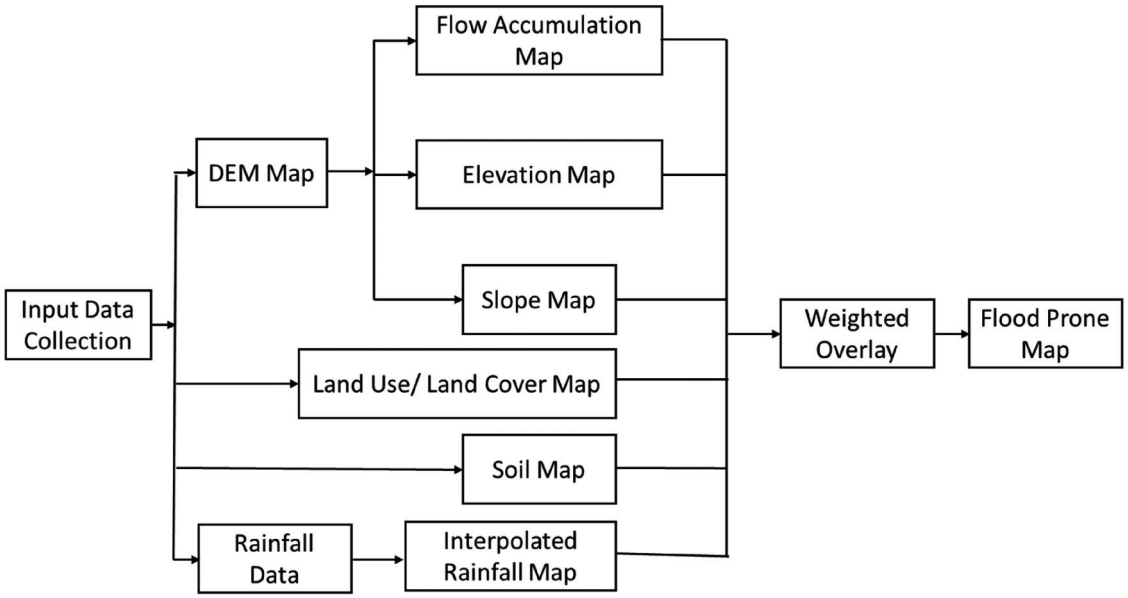

Figure 8. Flow chart of the methodology.

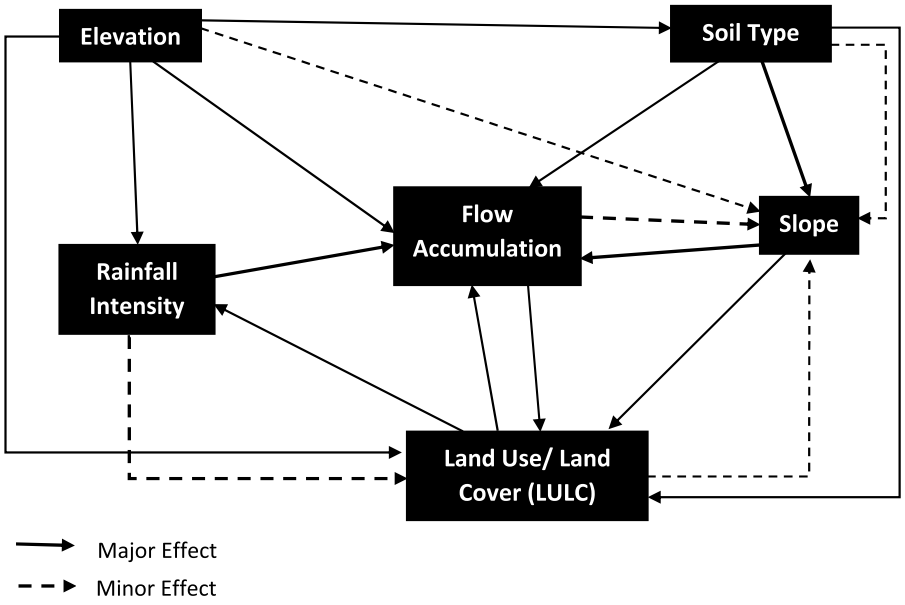

Figure 9. Flowchart of the major and minor effects of the factors affecting flood.

represent primary effects, where one factor directly impacts another. For instance, flow accumulation is shown to have a direct influence on land use, meaning it receives a primary effect score of one point. Dashed lines in Figure 8 represent secondary effects, indicating that one factor indirectly influences another. An example of this is how flow accumulation indirectly affects slope, receiving a secondary effect score of half a point. After identifying these effects, the scores for both primary and secondary interactions are summed to determine the overall weight of each factor. The total score for each factor reflects its significance in contributing to flood risk. Table 2 shows these calculated ratios, illustrating the relative impact of each factor.

The next step of this study involves combining the calculated rates with proposed weights to determine the overall weight for each factor influencing flood risk. This detailed assessment, expressed as a percentage, highlights the contribution of each factor to hazard-prone areas. Each factor's impact is classified into five hazard levels: very high, high, medium, low, and very low. While numeric factors such as flow accumulation, slope, elevation, and rainfall intensity are measured quantitatively, land use is evaluated descriptively. The Jenk's Natural Breaks method is employed to classify the numeric factors into five distinct hazard categories. This method allows for the statistical grouping of data points by identifying feature pairs with significant differences (Kourgialas and Karatzas 2011). It helps categorize the factors based on their flood hazard potential. For non-numeric factors like land use and soil maps, classifications are made based on their relative influence on flood risks. For example, areas with the lowest ratio of beneficial land use categories are marked as the most hazardous on the land use map. The final flood hazard map is produced by combining these factor maps using linear combinations and assigning appropriate weights to each. The six factors are categorized into different hazard levels, as detailed in Table 3, which

Table 2. Major and minor effects of the factors affecting flood risk analysis in Kaziranga National Park (Kourgialas and Karatzas 2011).

Sl. No.	Influencing Factors	Interactions of Factors	Rates	Outcomes
1	Land use/ Land Cover	2 major + 2 minor	(2 × 1) + (2 × 0.5) =	3.0 Points
2	Rainfall Intensity	1 major + 1 minor	(1 × 1) + (1 × 0.5) =	1.5 Points
3	Elevation	4 major + 1 minor	(4 × 1) + (1 × 0.5) =	4.5 Points
4	Soil Type	3 major + 0 minor	(3 × 1) + (0 × 0.5) =	3.0 Points
5	Flow Accumulation	1 major + 1 minor	(1 × 1) + (1 × 0.5) =	1.5 Points
6	Slope	2 major + 1 minor	(2 × 1) + (0 × 0.5) =	2.0 Points

assigns ratings for each level based on expert judgment. The hazard levels are rated as follows: 'Very High' = 10 points, 'High' = 8 points, 'Medium' = 5 points, 'Low' = 2 points, and 'Very Low' = 1 point. Once all the maps are prepared, a weighted linear combination approach is applied to assign percentage weights to each factor, with the total weight equalling 100%. This process results in a comprehensive map that identifies potential flood danger zones, providing valuable insights for flood risk management and decision-making. The categorization of factors ensures that areas most vulnerable to flooding are identified and addressed accordingly. By following this systematic weighting approach, the study ensures that the final flood risk map accurately represents the areas most prone to flooding, aiding in better planning and risk management.

After importing the different data layers into ArcMap, the next step involves organizing them into predefined classes. Once the layers are classified, the weights and ratios for each factor are combined to assess flood risk accurately. This is done by multiplying the ratio of each factor by the weight assigned to it. This method helps determine the overall impact of each factor on flood risk. For example, five distinct levels of flood risk are used in the analysis, each with a numerical value representing its hazard level. The total weight of each factor, which shows its influence on flood risk, is summarized in Table 3. The method assigns weights to parameters based on their relative importance in flood risk, determined using expert judgment, statistical analysis, or both. This approach prioritizes factors contributing significantly to flood risk (Narasayya 2021). Using the weighted sum method, normalized raster layers are multiplied by their assigned weights and summed to create a composite map, highlighting varying flood risk levels across locations. Flow accumulation values were categorized as follows using natural breaks in Arc GIS: Very High (398,937–612,826) with a weight of 10, High (230,710–398,937) with 8, Medium (88,919–230,710) with 5, Low (19,225–88,919) with 2, and Very Low (0–19,225) with 1. With one major and one minor interaction, the total rate for flow accumulation was 1.5. Multiplying the weights by this rate yielded a total weight of 39. Slope values were divided into Very High (0–3.30) assigned a weight of 10, High (3.30–8.50) with 8, Medium (8.50–17.47) with 5, Low (17.47–34.01) with 2, and Very Low (34.01–120.45) with 1. Two major interactions resulted in a total rate of 2. The total weight for the slope was calculated as 52. Land Use/Land Cover (LULC) categories included Very High (Water Bodies) with a weight of 10, High (Settlement) with 8, Medium (Barrenland) with 5, Low (Grassland) with 2, and Very Low (Forest Cover) with 1. Two major interactions gave a total rate of 3, resulting in a total weight of 78. Soil was classified into Very High to High (Orthic Acrisols) with a weight of 9, Moderate (Ferric Acrisols) with 5, and Low to Very Low (Dystric Nitosols) with 1.5. With three major interactions, the total rate was 3, giving a total weight of 46.5. Rainfall intensity in 2019 was

Table 3. Categorization and evaluation of the weighting of factors affecting flood-risk analysis in Kaziranga National Park.

Factors	Domain of effects	Descriptive LEVELS	Proposed Weight (a)	Rate (b)	Weighted Rate (a × b)	Total Weight	Percentage (%)
Flow Accumulation (pixels)	398937–612826	Very High	10	1.5	15	39	10.5
	230710–398937	High	8		12		
	88919–230710	Medium	5		7.5		
	19225–88919	Low	2		3		
	0–19225	Very Low	1		1.5		
Slope (%)	0–3.30	Very High	10	2	20	52	14
	3.30–8.50	High	8		16		
	8.50–17.47	Medium	5		10		
	17.47–34.01	Low	2		4		
	34.01–120.45	Very Low	1		2		
Land use/ Land Cover	Water bodies	Very High	10	3	30	78	21
	Settlement	High	8		24		
	Barrenland	Medium	5		15		
	Grassland	Low	2		6		
	Forest	Very Low	1		3		
Soil Type	Orthic Acrisols	Very High to High	9	3	27	46.5	12.52
	Ferric Acrisols	Moderate	5		15		
	Dystric Nitosols	Low to Very low	1.5		4.5		
Rainfall Intensity in 2019 (mm)	1000–2041	Very High	10	1.5	15	39	10.5
	500–1000	High	8		12		
	200–500	Medium	5		7.5		
	100–200	Low	2		3		
	0–100	Very Low	1		1.5		
Elevation (m)	27–72	Very High	10	4.5	45	117	31.49
	72–105	High	8		36		
	105–170	Medium	5		22.5		
	170–259	Low	2		9		
	259–431	Very Low	1		4.5		
Total						371.5	100

categorized as Very High (1000–2041 mm) with a weight of 10, High (500–1000 mm) with 8, Medium (200–500 mm) with 5, Low (100–200 mm) with 2, and Very Low (0–100 mm) with 1. One major and one minor interaction yielded a rate of 1.5, resulting in a total weight of 39. Elevation values ranged from Very High (27–72 m) with a weight of 10 to Very Low (259–431 m) with 1. Four major and one minor interaction gave a total rate of 4.5, resulting in a total weight of 117. Thus, the cumulative weight for all factors was calculated at 371.5, reflecting the combined impact of these parameters on flood risk. Based on the ratios provided in Table 3, the factors are combined with the following weights: flow accumulation (10.5%), slope (14%), land use (21%), rainfall intensity (10.5%), soil type (12.52%), and elevation (31.49%). These weights reflect how much each factor contributes to the likelihood of flooding in the area. A final flood hazard map is created by combining these factors using a weighted approach. This map highlights areas most at risk for flooding. The equation used to calculate this is shown as Equation (1), provided by Shaban *et al.* (2006):

$$F = \sum_{i=0}^{6} w_i x_i \quad (1)$$

where F indicates the final map of hazardous areas, w_i indicates the weight of factor i (%), and x_i indicates the rate of the factor i. Using GIS, the six thematic layers (flow accumulation, slope, land use, rainfall intensity, soil, and elevation) are combined with the help of the Model Builder tool. This tool enables efficient data integration to produce the flood hazard map, which helps identify high-risk flood areas in the research region.

Results and discussions

Results

Flooding significantly threatens forested areas, populated settlements, and productive farmlands within Kaziranga National Park (KNP). Given the park's history of frequent inundation, it is crucial to identify flood-prone locations to mitigate risks and enhance preparedness for future flood events. This study integrates multiple hydrological, topographical, and meteorological parameters, including flow accumulation, slope, land use, soil type, rainfall intensity, and elevation, to generate a comprehensive flood hazard map of KNP reflecting the weighted interaction rate of each factor. Out of these six parameters, the Digital Elevation Model (DEM) map of Kaziranga National Park, as illustrated in Figure 4, provides a crucial foundation for understanding the park's topographical variation. The elevation of KNP ranges from 27 meters to a maximum of 431 meters, with the highest elevations found in the southern region. To prepare the flow accumulation map, the DEM was processed using the 'Fill' tool in ArcGIS to remove depressions and ensure a continuous flow of water. The values of the Fill map range from 46 meters to 431 meters, reflecting the topographical adjustments made during processing. Following the 'Fill' process, the 'Flow Direction' map is created, which serves as a precursor to the final 'Flow Accumulation' map, as depicted in Figure 10(a). The values in the flow accumulation map range from 0 to 612,826, indicating regions where water is likely to converge, thereby identifying potential flood-prone zones. The slope plays a critical role in flood vulnerability; areas with lower slopes are more prone to flooding due to slower drainage and prolonged water retention. Therefore, a slope map is derived from the DEM, as shown in Figure 10(b).

Soil type is another crucial parameter that significantly affects flood susceptibility. Hence, a soil map is prepared for Kaziranga National Park, as shown in Figure 5. The soil map classifies the area into three dominant soil types: Dystric Nitosols, found in the elevated southern regions with well-drained properties; Orthic Acrisols, present in the central and northern parts, offering moderate drainage; and Ferric Acrisols, located in low-lying flood-prone areas with high water retention capacity. Now, a gridded rainfall map (Figure 8) is created for KNP using ten rainfall observation points within the study area. The rainfall data for 2015 and 2019 were acquired from the Climate Forecast System Reanalysis (CFSR). The maximum daily rainfall data recorded at 10 locations within the region are utilized to calculate the average annual rainfall using the IDW method, producing spatial rainfall distributions. Figure 11(a) shows the average annual rainfall map for 2015 of KNP. The rainfall values ranged from 1,487 mm to 1,916 mm. Higher rainfall was recorded in the northeastern part, moderate precipitation in the central region, and lower rainfall in the western section. Figure 11(b) shows the annual rainfall map for 2019 KNP. The rainfall values ranged from 1,831 mm to 2,041 mm, showing an overall increase compared to 2015. Similar spatial patterns persisted, with higher rainfall in the northeast and lower values in the west. As per the map, we can see that in 2019, there was slightly more rainfall than in 2015; therefore, more floods occurred in 2019.

Flood-prone maps for 2015 and 2019 are generated through a weighted overlay analysis of the six key parameters, as shown in Table 3. Figure 12 (a) presents the flood zone map for the year 2015. The flood risk values ranged from 130 to 470, with the highest flood-prone areas concentrated in low-lying regions. On the other hand, in 2019, flood risk values ranged from 115 to 480, indicating an overall increase in flood susceptibility over the four years. The comparative analysis (Table 4) reveals a noticeable increase in flood risk: in 2015, the very low and low flood-prone areas comprised 1.897% and 7.154% of the total area, respectively. Conversely, high and very high flood-prone areas accounted for 36.663% and 24.699%. By 2019, there was a slight increase in very low (1.926%) and low (8.152%) flood-prone areas. More critically, the high and very high flood-prone zones expanded to 36.834% and 31.263%, respectively. This data indicates a 7% increase in the 'very high' flood-prone zones, underscoring the escalating flood vulnerability of Kaziranga National Park (Figure 12a and b). The results suggest that increased rainfall and changes in hydrological conditions over time have exacerbated flood risks, particularly in low-lying regions.

Discussions

The study highlights a significant increase in flood risk in Kaziranga National Park from 2015 to 2019. The study effectively identifies the regions most prone to flooding

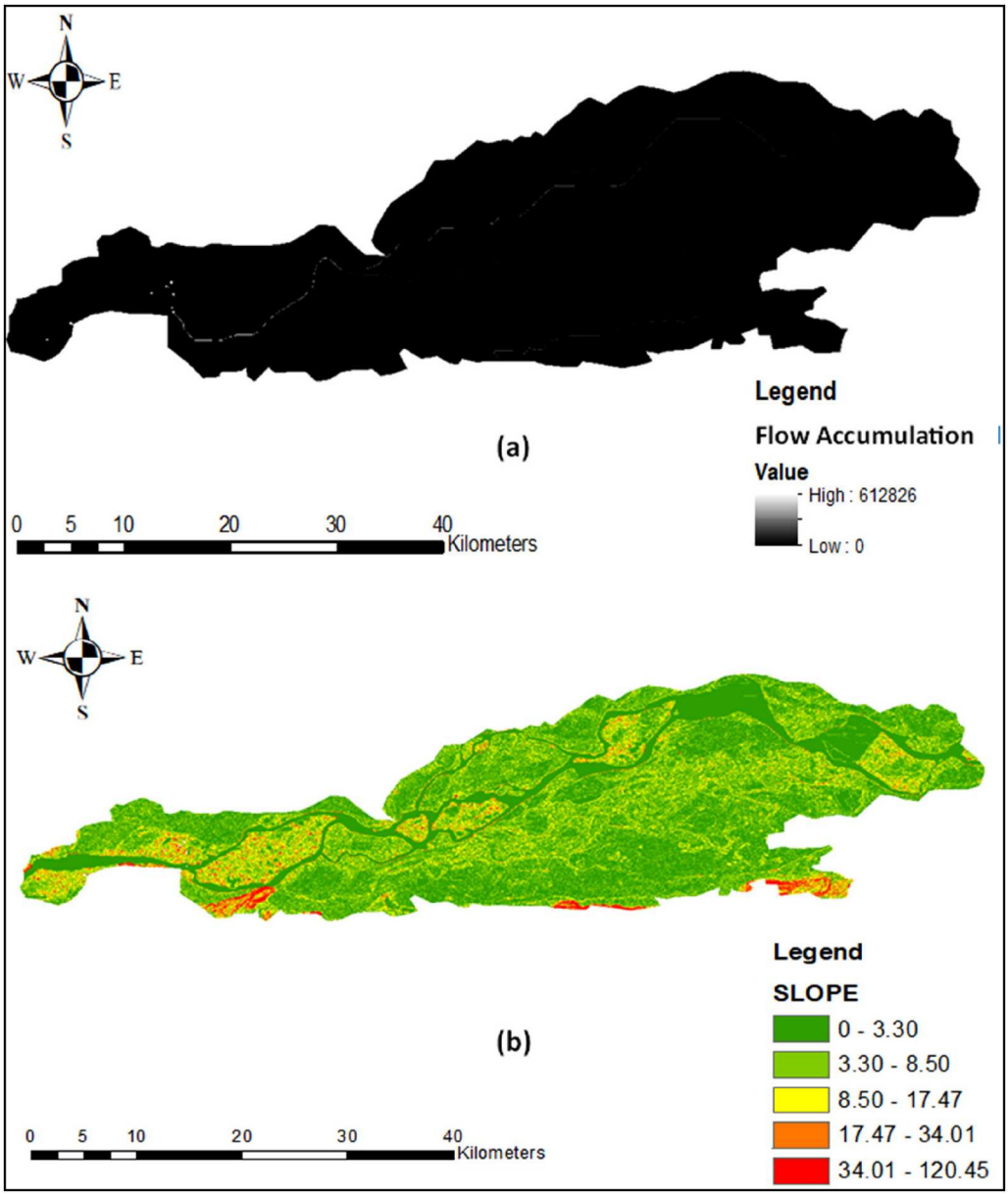

Figure 10. (a) Flow accumulation map and (b) Slope map of Kaziranga National Park (KNP).

and evaluates changes in flood risk over this period by analyzing key parameters such as flow accumulation, slope, land use, soil type, rainfall intensity, and elevation. One of the most significant observations is the change in rainfall patterns. The northeastern region consistently recorded the highest rainfall, whereas the western part received relatively lower precipitation. This increase in precipitation has played a crucial role in flood frequency and intensity, as higher rainfall contributes to more significant surface runoff and water accumulation in low-lying areas. The elevation analysis, derived from the Digital Elevation Model (DEM), reveals that flood-prone areas are primarily located in lower elevations closer to river channels, making them more susceptible to inundation during heavy rainfall events. The 'Flow Accumulation' map, generated using GIS-based hydrological modeling, further confirms that regions with high accumulation values align with flood-prone zones. These areas correspond to natural drainage pathways where water tends to concentrate. The analysis of soil types, in particular, adds a valuable dimension to flood risk assessment. The regions at higher flood risk predominantly feature Acrisol soil – a clayey soil with poor infiltration properties. Acrisols have a low infiltration rate, which limits their capacity to absorb water during rainfall events, resulting in greater surface runoff and increased flood potential. The combination of these soil characteristics with higher rainfall intensity in 2019 contributed significantly to the expansion of flood-prone areas. This highlights the critical role of soil properties in flood susceptibility, which is often overlooked in many flood hazard studies. The slope plays a critical role in flood vulnerability; areas with lower slopes are more prone to flooding due to slower drainage and prolonged water retention. Conversely, steeper slopes facilitate rapid runoff, reducing the likelihood of standing water. Low-lying and level areas have a higher danger of flooding. Flood-prone maps for 2015 and 2019, developed using weighted overlay analysis, illustrate the growing flood risk in KNP. The increase in flood-prone areas is attributed to multiple factors, including increased precipitation, topographical characteristics, and possible land use changes. The northeastern region, which experienced the highest increase

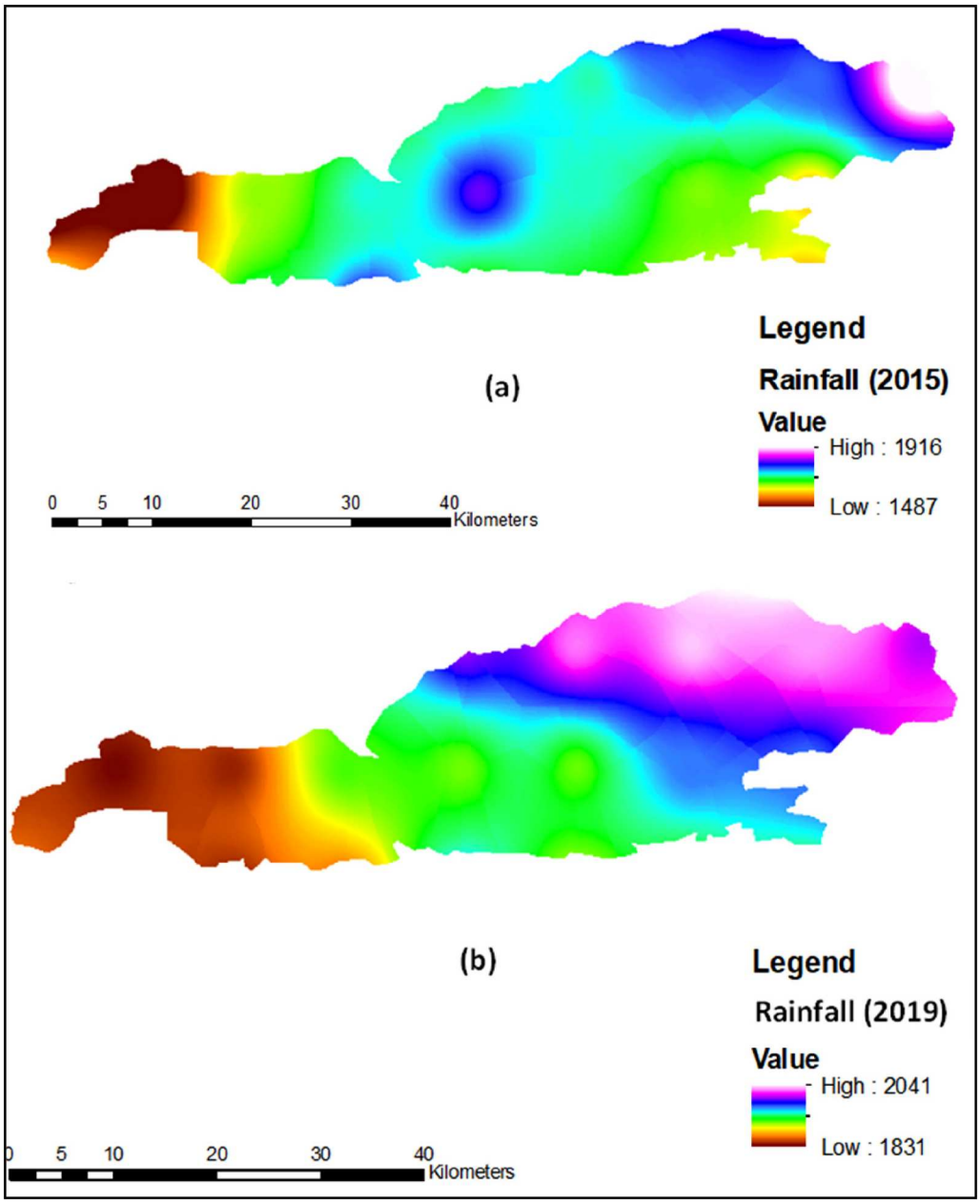

Figure 11. Average annual rainfall maps for the years (a) 2015 and (b) 2019 in Kaziranga National Park (KNP).

in rainfall intensity, also witnessed the most significant expansion in flood-prone zones. Additionally, changes in river morphology, sediment deposition, embankment breaches, and anthropogenic activities such as deforestation and agricultural expansion may have further altered the hydrological responses within KNP. This study highlights the strong correlation between rainfall intensity and flood-prone areas, emphasizing how climatic factors, including increased rainfall driven by climate change, exacerbate flood hazards alongside topographical and hydrological influences. The temporal analysis underscores how shifting climatic patterns, such as heightened precipitation intensity and frequency, are driving the expansion of high-risk flood-prone zones. Furthermore, it underscores the importance of integrating climate change considerations with regional policies and global flood management trends. While the findings emphasize the significant role of flooding in wildlife displacement, mortality, and human-wildlife conflict, similar studies corroborate these observations and provide additional dimensions to the problem. For instance, Talukdar (2022) highlighted that over 90% of Kaziranga's area gets submerged during severe floods, aligning with this study's findings on extensive habitat inundation. Though the method is widely applied in different studies but this method doesn't explore potential mitigation infrastructure in depth. The present study need more emphasis on anthropogenic influences beyond deforestation. Although the GIS-based approach and temporal data analysis demonstrated in this study provide a replicable framework for tracking flood risk changes over time, enhancing resilience in the face of evolving climatic and environmental pressures. Thus, the results emphasize the urgent need for enhanced flood management and mitigation strategies in Kaziranga National Park. Given its status as a UNESCO World Heritage site and home to several endangered species, including the Indian rhinoceros, conservation efforts must incorporate flood risk assessment with sustainable land management practices.

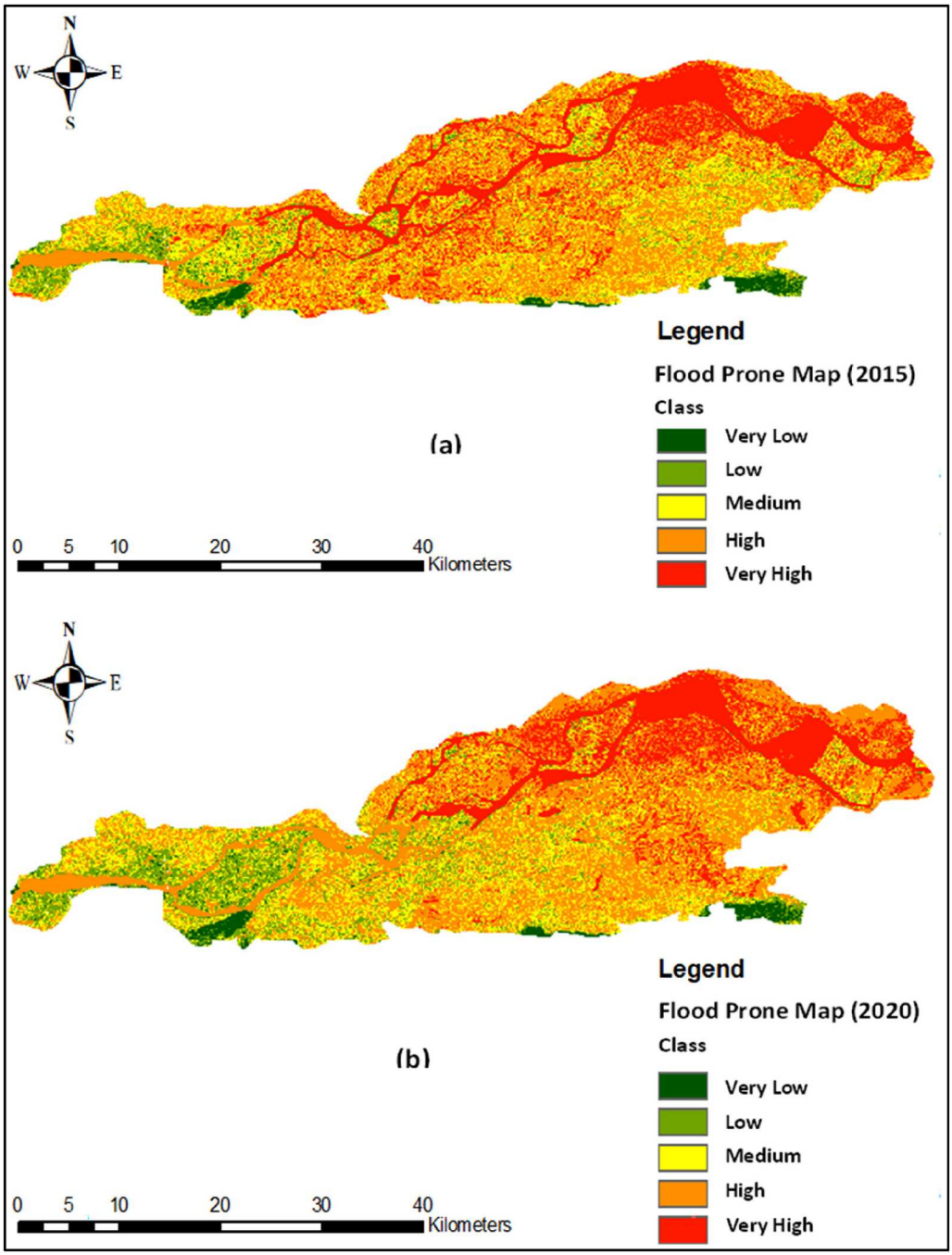

Figure 12. Flood-prone maps of Kaziranga National Park for (a) 2015 and (b) 2019.

Table 4. Flood risk analysis classes for Kaziranga National Park.for the years 2015 and 2019 with their values.

		2015			2019		
Sl. No.	Classes	Values	Area (km^2)	Area (%)	Values	Area (km^2)	Area (%)
1	Very Low	130–250	20.577	1.897	115–250	20.993	1.926
2	Low	250–315	77.978	7.154	250–315	88.856	8.152
3	Medium	315–360	322.465	29.584	315–360	237.859	21.822
4	High	360–400	399.626	36.663	360–400	401.490	36.834
5	Very High	400–470	269.219	24.699	400–480	340.734	31.263

Conclusions

The present study involved the creation of a flood hazard zone map for Kaziranga National Park in India, employing flow accumulation, elevation, soil type, LULC, rainfall intensity, and slope parameters. This research examined six criteria based on terrain, climate, soil type, and land use information. After computing the weights, the final flooding-prone map was created using Arc GIS software. The research area, which was shown as the darkest area, had the greatest risk of flooding. However, as the areas became lighter, the likelihood of flooding diminished. Additional validation was carried out to ensure the outcome. This outcome might be a valuable tool for determining flood danger. Due to the presence of flat and impermeable regions, the northeastern portion of Kaziranga National Park is more

vulnerable to flooding than the western portion. The model's outcomes provide a detailed representation of the flooding hazard in Kaziranga National Park, with 'very low', 'low', 'moderate', 'high', and 'very high' flooding risk zones, respectively, for the national park in 2015 and 1.89%, 7.15%, 29.58%, 36.66%, and 24.69% in 2019. The summarized findings can be outlined as follows:

(1) The inundation area derived from the method reveals that flood values range from 130 to 470 for 2015 and from 115 to 480 for 2019 in the flood plains and along the river. Additionally, the total flooded area measures 668.84 sq. km and 742.22 sq. km for 2015 and 2019, respectively.
(2) The flood hazard analysis indicates that the majority of the area falls within the high-hazard category.
(3) The areas most affected by the flood were forests with lower elevations and some agricultural lands.
(4) The most dominant factors affecting flood risk are found to be rainfall intensity, soil type, and elevation.

The current research identified specific locations with high or low flood risk. This will be crucial in aiding decision-makers in the planning and mitigation of flooding. The findings of this study can reduce the harm that flood catastrophes offer to the animal population in the studied region. Few recommendations to be given to reduce flood risks in Kaziranga are as follows:

(1) By prioritizing reinforcing embankments, constructing flood relief channels, and improving drainage systems.
(2) By establishing early warning systems and build elevated wildlife shelters to protect vulnerable species.
(3) By restoring floodplain habitats and promote flood-resistant infrastructure. This study intends to suggest the creation of artificial highlands within Kaziranga National Park as a possible solution.
(4) Engage local communities in flood preparedness and sustainable farming to reduce runoff, preserving wildlife and livelihoods. Furthermore, adopting adaptive land-use planning, water resource management, and soil conservation practices can reduce vulnerability to future floods.
(5) The study's findings can guide local officials in communicating risks and devising mitigation strategies.
(6) Ensure meteorological agencies provide seasonal forecasts and climate predictions to facilitate effective flood management plans.
(7) Risk maps will support environmental impact assessments and address why communities build on floodplains.

Expand the study to analyze advanced computational tools for forecasting flood risks, enhancing preparedness, and reducing vulnerability for high-risk areas, safeguarding both residents and wildlife. Future work in this area will concentrate on automating the process by transferring the various classification systems from ArcGIS Pro into Python. The method's results, which require validation against historical flood occurrences spanning several years and covering the entire designated Kaziranga National Park, expose the technical limitations of the approach. Future studies should prioritize integrating satellite-based rainfall data, hydrological modeling, and citizen science for data collection. The uncertainties in the evaluation of data may arise as proportion of the weighted elements varies from study area to study area and is not consistent (Meresa, 2022). The lack of stream flow gauges and short-interval rainfall readings may have an impact on the method's findings. Despite the mentioned limitations, the model would serve as a valuable tool for mapping and assessing flood risk events if its results could be validated against other models and real flood occurrences. Future research should explore extending the weighted overlay methodology to other flood-prone regions and incorporate socio-economic factors, such as community resilience, to refine flood risk assessments and conservation strategies.

Availability of data and material

The data used for this work has been included in the manuscript.

Disclosure statement

No potential conflict of interest was reported by the author(s).

Notes on contributors

Dr. Shehnaj Ahmed Pathan is an Assistant Professor in the Department of Civil Engineering at The Assam Kaziranga University. She holds M.Tech. and Ph.D. degrees in Water Resources Engineering from the National Institute of Technology, Silchar. Her research area focuses on Hydrology, with experience in Rainfall, Soil Erosion and Sediment data analysis, Remote Sensing, GIS, Hydrological Modelling, etc.

Mr. Gwakulo Tep, received his B.Tech. in Civil Engineering and M.Tech. in Water Resources Engineering both from The Assam Kaziranga University. His B.Tech. project focused on the filtration of water using a traditional method of filtration. His present research mainly focuses on Flood analysis, GIS and Remote Sensing.

References

Adlyansah, A.L., Husain, L.R., and Pachri, H., 2019. Analysis of flood hazard zones using overlay method with figused-based scoring based on geographic information systems: case study in parepare city South Sulawesi province. *OP Conference Series: Earth and Environmental Science,*, 280 (1), 012003.

Ajjur, S.B. and Mogheir, Y.K., 2020. Flood hazard mapping using a multi-criteria decision analysis and GIS (case study Gaza Governorate, Palestine). *Arabian Journal of Geosciences*, 13, 1–11.

Ashwini, K., Pathan, S.A., and Sil, B.S., 2020. Delineation of groundwater potential zone and flood risk zone in Cachar District area, India. *Journal of Water Engineering and Management*, 1, 16–34.

Assefa, T.H., 2018. Flood risk assessment in Ethiopia. *Civil and Environmental Research*, 10 (1), 35–40.

Babalola, A.M. and Abilodun, O.K., 2019. Assessment of road vulnerability to flood: a case study. *International Journal of Engineering Science*, 7, 45–50.

Bapalu, G.V. and Sinha, R., 2005. GIS in flood hazard mapping: a case study of Kosi River Basin, India. *GIS Development Weekly*, 1 (13), 1–3.

Bartalev, S.A., *et al.*, 2003. A new SPOT4-VEGETATION derived land cover map of Northern Eurasia. *International Journal of Remote Sensing*, 24 (9), 1977–1982.

Barua, M. and Sharma, P., 1999. Birds of Kaziranga National Park, India. In: M. Barua, ed. *Forktail*. Guwahati: Barua Bhavan, 47–60.

Belmonte, A.M.C. and Beltrán, F.S., 2001. Flood events in Mediterranean ephemeral streams (ramblas) in Valencia region. *Spain. Catena*, 45 (3), 229–249.

Bento, A.M., *et al.*, 2023. Improved assessment of maximum streamflow for risk management of hydraulic infrastructures. A case study. *International Journal of River Basin Management*, 21 (3), 489–499.
Borah, S.B., et al., 2018. Flood inundation mapping and monitoring in Kaziranga National Park, Assam using Sentinel-1 SAR data. *Environmental monitoring and assessment*, 190 (9), 520.
Eini, M., *et al.*, 2020. Hazard and vulnerability in urban flood risk mapping: machine learning techniques and considering the role of urban districts. *International Journal of Disaster Risk Reduction*, 50, 101687.
Emmanuel Udo, A., *et al.*, 2015. Flood hazard analysis and damage assessment of 2012 flood in Anambra State using GIS and remote sensing approach. *American Journal of Geographic Information System*, 4 (1), 38–51.
Enomah, L.D., *et al.*, 2024. Flood risk assessment in Limbe (Cameroon) using a GIS weighed sum method. *Environment, Development and Sustainability*, 26 (11), 29725–29744.
Erena, S.H. and Worku, H., 2018. Flood risk analysis: causes and landscape based mitigation strategies in Dire Dawa city, Ethiopia. *Geoenvironmental Disasters*, 5, 1–19.
Fagunloye, O.C., 2024. Mapping of flood risk zones using multi-criteria approach and radar a case study of Ala and Akure-Ofosu communities, Ondo State, Nigeria. *International Journal of Geosciences*, 15, 605–631.
Ghosh, S., *et al.*, 2018. Assessment of flood-emanated impediments to Kaziranga National Park Grassland Ecosystem—a binocular vision with remote sensing and geographic information system. In: C.S. Singh, ed. *Geospatial applications for natural resources management*. Boca Raton: CRC Press, 275–290.
Ghosh, A., *et al.*, 2023. Flood hazard mapping using GIS-based statistical model in vulnerable riparian regions of sub-tropical environment. *Geocarto International*, 38 (1), 2285355.
Hagos, Y.G., *et al.*, 2022. Flood hazard assessment and mapping using GIS integrated with multi-criteria decision analysis in upper Awash River basin, Ethiopia. *Applied Water Science*, 12 (7), 148.
Hasanloo, M., Pahlavani, P., and Bigdeli, B., 2019. Flood risk zonation using a multi-criteria spatial group fuzzy-ahp decision making and fuzzy overlay analysis. *The International Archives of the Photogrammetry, Remote Sensing and Spatial Information Sciences*, XLII-4/W18, 455–460.
James, L.D. and Hall, B., 1986. Risk information for floodplain management. *Journal of Water Resources Planning and Management*, 112 (4), 485–499.
Kourgialas, N.N. and Karatzas, G.P., 2011. Flood management and a GIS modelling method to assess flood-hazard areas—a case study. *Hydrological Sciences Journal*, 56 (2), 212–225.
Kron, W., Löw, P., and Kundzewicz, Z.W., 2019. Changes in risk of extreme weather events in Europe. *Environmental Science & Policy*, 100, 74–83.
Kumar, N. and Jha, R., 2023. GIS-based flood risk mapping: the case study of Kosi River Basin, Bihar, India. *Engineering, Technology & Applied Science Research*, 13 (1), 9830–9836.
Kumar, G.P. and Sen, S.D., 2022. Flood hazard and risk assessment of Deoha River Basin, Central Ganga Plain, India: an GIS approach. *Disaster Advances*, 15 (10), 42–51.
Kushwaha, S.P.S., *et al.*, 2000. Land area change and rhino habitat suitability analysis in Kaziranga National Park, Assam. *Tigerpaper*, 27 (2), 9–17.
Kushwaha, S.P.S. and Unni, N.M., 1986. Application of remote sensing techniques in forest cover monitoring and habitat evaluation. A case study in Kaziranga National Park, Assam. *In*: *Proceedings of seminar-cum-workshop on wildlife habitat evaluation using remote sensing techniques*. Dehradun: Indian Institute of Remote Sensing/Wildlife Institute of India, 238–247.
Malgwi, M.B., Schlögl, M., and Keiler, M., 2021. Expert-based versus data-driven flood damage models: a comparative evaluation for data-scarce regions. *International Journal of Disaster Risk Reduction*, 57, 102148.
Mase, L.Z., 2020. Slope stability and erosion-sedimentation analyses along sub-watershed of Muara Bangkahulu River in Bengkulu City, Indonesia. *E3S Web of Conferences*, 148 (5), 03002.
Mathur, V.B., *et al.*, 2005. Opportunities and challenges for Kaziranga National Park, Assam over the next fifty years. *UNF-UNESCO Enhancing Our Heritage Project Team*, 1 (1), 1–15.
Medhi, S. and Sakia, M.K., 2019. Spatial relationship between mother-calf of Rhinoceros unicornis.
Meresa, H., *et al.*, 2022. The role of input and hydrological parameters uncertainties in extreme hydrological simulations. *Natural Resource Modeling*, 35 (1), e12320.
Mohammed, Z.T., Hussein, L.Y., and Abood, M.H., 2024. Potential flood hazard mapping based on GIS and analytical hierarchy process. *Journal of Water Management Modeling*, 32, 1–26.
Narasayya, K., 2021. A study on flood hazard zonation mapping based on GIS-driven approach using remote sensing data and weighted overlay analysis (WOA) model. *International Journal for Multidisciplinary Research (IJFMR)*, 6 (5), 1–15.
Osman, S.A. and Das, J., 2023. GIS-based flood risk assessment using multi-criteria decision analysis of Shebelle River Basin in Southern Somalia. *SN Applied Sciences*, 5 (5), 134.
Ouma, Y.O. and Tateishi, R., 2014. Urban flood vulnerability and risk mapping using integrated multi-parametric AHP and GIS: methodological overview and case study assessment. *Water*, 6 (6), 1515–1545.
Ozkan, S.P. and Tarhan, C., 2016. Detection of flood hazard in urban areas using GIS: Izmir case. *Procedia Technology*, 22, 373–381.
Patnaik, N.D., Sharma, K., and Chaudhry, P., 2019. Kaziranga National Park of India: ome wildlife and tourism management related pressing issues. *Jharkhand Journal of Development and Management Studies*, 17 (2), 8127–8141.
Rodger, W.A., Panwar, H.S., and Mathur, V.B., 2002. Wildlife protected area network in India: a review. In: S. Shrotriya, ed. *Wildlife institute of India*. Dehradun: Wildlife Institute of India, 1–51.
Shaban, A., *et al.*, 2001. Assessment of road instability along a typical mountainous road using GIS and aerial photos, Lebanon – Eastern Mediterranean. *Bulletin of Engineering Geology and the Environment*, 60, 93–101.
Shaban, A., Khawlie, M., and Abdallah, C., 2006. Use of remote sensing and GIS to determine recharge potential zones: the case of Occidental Lebanon. *Hydrogeology Journal*, 14, 433–443.
Sinha, R., *et al.*, 2008. Flood risk analysis in the Kosi River Basin, North Bihar using multi-parametric approach of analytical hierarchy process (AHP). *Journal of the Indian Society of Remote Sensing*, 36, 335–349.
Sinha, S.P., Sinha, B.C., and Qureshi, Q., 2011. *The Asiatic one-horned rhinoceros (Rhinoceros unicornis) in India and Nepal: ecology, management and conservation strategies*. Switzerland: Lambert Academic Publishing. http://www. rhinoresourcecenter. com/pdf_files/13, 8, 1386490749.
Svoboda, A., 1991. Changes in flood regime by use of the modified curve number method. *Hydrological Sciences Journal*, 36 (5), 461–470.
Talukdar, B.K., 2022. Asian Rhino specialist group chair report/ rapport du groupe de spécialistes du rhinocéros d'Asie. *Pachyderm*, 63, 33–37.
Thapa, S., *et al.*, 2020. Catchment-scale flood hazard mapping and flood vulnerability analysis of residential buildings: the case of Khando River in eastern Nepal. *Journal of Hydrology: Regional Studies*, 30, 100704.
Wang, Y., *et al.*, 2011. A GIS-based spatial multi-criteria approach for flood risk assessment in the Dongting Lake Region, Hunan, Central China. *Water Resources Management*, 25, 3465–3484.